

Memory-multi-fractional Brownian motion with continuous correlations

Wei Wang,¹ Michał Balcerak,² Krzysztof Burnecki,² Aleksei V. Chechkin,^{1, 2, 3} Skirmantas Janušonis,⁴ Jakub Ślęzak,² Thomas Vojta,⁵ Agnieszka Wyłomańska,² and Ralf Metzler^{1, 6}

¹*Institute of Physics & Astronomy, University of Potsdam, 14476 Potsdam, Germany*

²*Faculty of Pure and Applied Mathematics, Hugo Steinhaus Center, Wrocław University of Science and Technology, Wrocław, Poland*

³*Akhiezer Institute for Theoretical Physics, National Science Center*

⁴*Kharkov Institute of Physics and Technology", Kharkov 61108, Ukraine*

⁵*Department of Psychological and Brain Sciences, University of California, Santa Barbara, Santa Barbara, CA 93106, USA*

⁵*Department of Physics, Missouri University of Science and Technology, Rolla, MO 65409, USA*

⁶*Asia Pacific Center for Theoretical Physics, Pohang 37673, Republic of Korea*

(Dated: 6th March 2023)

We propose a generalization of the widely used fractional Brownian motion (FBM), memory-multi-FBM (MMFBM), to describe viscoelastic or persistent anomalous diffusion with time-dependent memory exponent $\alpha(t)$ in a changing environment. In MMFBM the built-in, long-range memory is continuously modulated by $\alpha(t)$. We derive the essential statistical properties of MMFBM such as response function, mean-squared displacement (MSD), autocovariance function, and Gaussian distribution. In contrast to existing forms of FBM with time-varying memory exponents but reset memory structure, the instantaneous dynamic of MMFBM is influenced by the process history, e.g., we show that after a step-like change of $\alpha(t)$ the scaling exponent of the MSD after the α -step may be determined by the value of $\alpha(t)$ before the change. MMFBM is a versatile and useful process for correlated physical systems with non-equilibrium initial conditions in a changing environment.

PACS numbers: 87.15.Vv, 87.16.dp, 82.56.Lz, 05.40.-a, 02.50.-r

The stochastic motion of individual colloidal particles or labeled single molecules is routinely recorded by single-particle tracking [1] in soft- and bio-matter systems [2–4], i.a., crowded liquids [5, 6], cytoplasm of biological cells [7–11], actively driven tracers [12–14], lipid membranes [15–17], and porous media [18]. In silico, lipid and protein motion [19–21] or internal protein dynamics [21, 22] are sampled. On larger scales, motile cells or small organisms [23–25], and animals, e.g., marine predators or birds [26–30] are traced. Often the observed motion deviates from Brownian motion with its linear mean-squared displacement (MSD) $\langle x^2(t) \rangle \simeq t$ and Gaussian displacement probability density function (PDF) [31]. Instead, anomalous diffusion with MSD $\langle x^2(t) \rangle \simeq t^\alpha$ emerges [2–4], with sub- ($0 < \alpha < 1$) and superdiffusion ($\alpha > 1$) [2, 32]. Depending on the system, anomalous diffusion is described by different generalized stochastic models [32–36].

Two such processes have turned out to be particularly suited to model anomalous diffusion in a wide range of systems. One is the continuous time random walk, in which (waiting) times τ between two successive jumps are randomly distributed [32–34]. When the PDF of τ has the scale-free form $\psi(\tau) \simeq \tau^{-1-\alpha}$ with $0 < \alpha < 1$, the resulting motion is subdiffusive [32–34]. Power-law forms for $\psi(\tau)$ were, i.a., measured for colloids in actin gels [37, 38], membrane channels [15], doxorubicin molecules in silica slits [39], ribonucleoproteins in neurons [40], foraging birds [30], or in weakly chaotic systems [41, 42].

The second common anomalous diffusion process is fractional Brownian motion (FBM) [43, 44] based on

the stochastic equation $dX(t)/dt = \xi(t)$ driven by fractional Gaussian noise (FGN) with stationary autocovariance function (ACVF) $\langle \xi(t)\xi(t+\tau) \rangle \sim \frac{1}{2}\alpha(\alpha-1)K_\alpha\tau^{\alpha-2}$ ($0 < \alpha \leq 2$) [45, 46]. Then, $\langle X^2(t) \rangle \simeq K_\alpha t^\alpha$ with the generalized diffusivity K_α of dimension length²/time ^{α} . The ACVF is negative (“antipersistent”) for subdiffusion and positive (“persistent”) for superdiffusion. Displacement ACVFs consistent with sub- and superdiffusive FBM were identified, i.a., for tracers in crowded liquids [5–9, 47–50], doxorubicin [39], lipids [19], amoeba motion [47, 48], and cruising birds [30]. Specifically, subdiffusive FBM models diffusion in viscoelastic systems (cellular cytoplasm, crowded liquids) [5–9, 19], or “roughness” in finance [51, 52]. FBM is intrinsically Gaussian [43–45], yet, in several viscoelastic systems non-Gaussian displacement PDFs were found [8, 16, 20, 49, 50]. This phenomenon (similar to Brownian yet non-Gaussian diffusion [53, 54]) was ascribed to the systems’ heterogeneity and modeled by superstatistical viscoelastic motion [55], FBM switching between two diffusivities [49] or featuring a stochastic (“diffusing” [56, 57]) diffusivity [58, 59], and subordinated FBM [50]. Random anomalous memory exponents α were studied in particle ensembles [60, 61].

Here we address systems in which the properties of long-range correlated motions do not vary stochastically but the memory exponent α changes deterministically over time, $\alpha(t)$. Examples include smoothly changing viscoelastic environments, e.g., during biological cell cycles [62], or when pressure and/or concentrations are changed in viscoelastic solutions [63, 64]. $\alpha(t)$

may switch more abruptly when the test particle moves across boundaries to a different environment. Jump-like changes of α may be effected by binding to larger objects or surfaces [49, 65] or multimerization [65, 66] of the tracer. Drops in α from superdiffusion with $\alpha \approx 1.8$ to strong subdiffusion $\alpha \approx 0.2$ of intracellular particles were effected by blebbistatin treatment knocking out active molecular motor action in amoeba cells; after some time, the positive correlations and thus superdiffusion were restored [47]. Cellular sub-micron or micron-sized “cargo” transported by molecular motors may switch between motor-driven transport and rest phases, effecting repeated sub/superdiffusive switches [67, 68]. Finally, crossovers between sub/superdiffusive modes as well as changes in exponents within sub- or superdiffusion may occur for (intermittent) search of birds or other animals. We model such situations by a specified protocol $\alpha(t)$ for the memory exponent in our memory-multi-FBM (MMFBM) model, in which the memory of MMFBM is continuously modulated by $\alpha(t)$. Due to the uninterrupted memory, the instantaneous dynamic of MMFBM is influenced by the full history of the process. We study these memory effects on trajectories, response function, MSD, and ACVF. We show that MMFBM is Gaussian and discuss relations to other generalized FBM models.

To motivate our approach, consider the simple case of a Brownian particle with diffusivity K_1 , released at time $t = 0$. At time $t = \tau$ it switches to a new diffusivity K_2 , e.g., by crossing to a different environment, multimerization [66], or conformational changes [21]. The MSD of this particle has the form $\langle x^2(t) \rangle = 2K_1t$ for $t \leq \tau$ and $= 2K_2(t - \tau) + 2K_1\tau$ for $t > \tau$. A convenient way to formulate such types of processes is based on the Wiener process $B(t)$ [31] using $\tilde{B}(t) = \int_0^t \sqrt{K(s)} dB(s)$. In this formulation $K(s)$ continuously modulates the Wiener increments $dB(s)$ and, e.g., leads to above MSD.

In a similar fashion we incorporate a time-dependent memory exponent $\alpha(t)$ in FBM. For a physical process initiated at $t = 0$ we use Lévy’s formulation [69] of non-equilibrated FBM in terms of a (Holmgren) Riemann-Liouville fractional integral (RL-FBM) [44, 70],

$$X(t) = \int_0^t \sqrt{\alpha(s)}(t-s)^{(\alpha(s)-1)/2} dB(s). \quad (1)$$

In standard RL-FBM, the power-law memory kernel with constant exponent α modulates the Wiener increments $dB(s)$ along the path and at long times is equivalent to integrated FGN. Thus, at any point the process $X(t)$ depends on its full history. For $\alpha = 1$ the kernel vanishes and $X(t)$ is Brownian motion [44]. For changing environments MMFBM incorporates these changes locally into the memory function, i.e., by variation of how the correlations of the Wiener increments $dB(s)$ are modulated by $\alpha(s)$ along the path. Thus the uninterrupted history of $\alpha(t)$ is contained yet the strength of the memory varies throughout the process history. We note that due to the

explicit time dependence of $\alpha(t)$ the noise ACVF is not stationary by construction. We also note that the structure (1) for $X(t)$ is similar to time-fractional dynamics of CTRWs with scale-free waiting time PDF [33] and extensions to variable-order with time-dependent memory exponent [71]. We show that MMFBM with its statistical observables is a meaningful generalization of FBM.

Response function. We consider MMFBM (1), that is originally Brownian (i.e., $\alpha = 1$) up to time τ and then experiences a short period δ with exponent $\alpha \neq 1$. After $t = \tau + \delta$, the process is again Brownian. With the increments $X^\delta(\tau) = X(\tau + \delta) - X(\tau)$ the response function is

$$\langle X^\delta(\tau)X^\delta(\tau+T) \rangle = \alpha \frac{\alpha - 1}{2T^{1-\alpha}} \delta \mathbb{B} \left(\frac{\delta}{T}; \frac{\alpha + 1}{2}, 1 - \alpha \right) \quad (2)$$

for $\delta \rightarrow 0$, at time T after start of the perturbation with α [72]. \mathbb{B} is the incomplete Beta function. When $T \rightarrow \infty$, $\langle X^\delta(\tau)X^\delta(\tau+T) \rangle \sim \alpha[(\alpha - 1)/(\alpha + 1)]\delta^{\alpha/2+3/2}T^{\alpha/2-3/2}$. Thus, even after a long period T a short perturbation still influences the process, and the sign of (2) depends on whether $\alpha \geq 1$. For $\alpha = 1$ (2) is zero, as expected.

In fact, MMFBM (1) is formally similar to definitions in continuous and discrete time of multifractional FBM (MFBM)[73–76], a diverse family of processes based on a deterministic $\alpha(t)$ [77, 78]. MFBM and dedicated testing algorithms [79, 80] is used to describe data traffic dynamics [81, 82], financial time series [83], turbulent dynamics [84], or consumer index dynamics [85]. In most MFBM formulations, it is of interest to describe the roughness of trajectories and have a globally changing scaling exponent of the MSD. This is achieved by replacing $\alpha(s)$ in (1) by $\alpha(t)$, i.e., the Wiener increments $dB(s)$ at time t are modulated by the same exponent throughout the “history”. When $\alpha(t)$ changes, the memory of the correlations is reset and globally replaced by a new weight [86]. The changes of $\alpha(t)$ in MFBM directly affect the MSD, which scales as $\langle x^2(t) \rangle \simeq t^{\alpha(t)}$. This can be directly seen when calculating the response function: for MFBM (2) is identically zero, i.e., the reset of the history in MFBM kills any influence of the perturbation even at short periods T . We discuss further differences between MMFBM and MFBM below, arguing that MMFBM reflects memory properties expected for long-range correlated dynamics with uninterrupted memory.

Step-wise $\alpha(t)$ -protocol. To simplify the discussion of the general properties of MMFBM, we consider a step-wise protocol between two values of α switching at $t = \tau$,

$$\alpha(t) = \begin{cases} \alpha_1, & t \leq \tau \\ \alpha_2, & t > \tau \end{cases}, \quad (3)$$

in an unbounded space. More complicated behaviors can be constructed as a sequence of values α_i . Smooth versions of the step-like protocol (3) can, e.g., be realized by sigmoid functions (S17) [72]. Such forms, however,

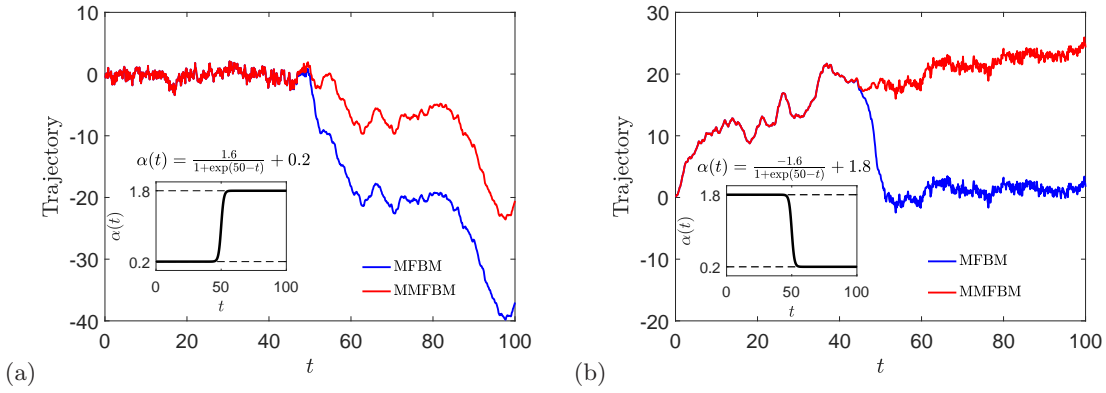


Figure 1: Sample trajectories for MMFBM (1) (red) and MFBM (S6) (blue) for sigmoid protocol (see legend) for $\alpha(t)$ with switching time $\tau = 50$ and (a): $\alpha_1 = 0.2$, $\alpha_2 = 1.8$; (b): $\alpha_1 = 1.8$, $\alpha_2 = 0.2$. In each panel both trajectories are based on the same realization of the parental Wiener process. For step-like protocol (3) see Fig. S1.

require numerical analysis. Fig. 1 shows trajectories of MMFBM for the smooth versions corresponding to two sample protocols (3), while Fig. S1 depicts the case for the step-like form (3) [72]. In both Figures we also show the corresponding MFBM trajectories, for the same parental Wiener processes $B(s)$. For both processes the roughness change in the trajectories at $t = \tau$ is distinct. In both cases MMFBM appears more ‘‘continuous’’.

MSD. With definition (1), the MMFBM-MSD reads

$$\langle X^2(t) \rangle = \int_0^t \alpha(s)(t-s)^{\alpha(s)-1} ds, \quad (4)$$

due to the independence of the Wiener process at different times. Indeed, the instantaneous value of the MSD depends on the local modulation by $\alpha(s)$ along the process history. For the stepwise protocol (3), the MSD reads

$$\langle X^2(t) \rangle = \begin{cases} t^{\alpha_1}, & t \leq \tau \\ t^{\alpha_1} - (t-\tau)^{\alpha_1} + (t-\tau)^{\alpha_2}, & t > \tau \end{cases}. \quad (5)$$

This form contrasts the MFBM result, for which $\langle X^2(t) \rangle \propto t^{\alpha(t)}$ for all t , i.e., for step-change (3) of α the MSD scaling exponent changes abruptly from α_1 to α_2 at $t = \tau$: by memory reset, at time t the history of the previous memory exponents at $s < t$ is erased in MFBM [72, 77, 78]. We note that in MMFBM even for stepwise $\alpha(t)$ considered here, the MSD is continuous at $t = \tau$ (the derivative is continuous for strong memory, $\alpha_1, \alpha_2 > 1$).

The MSD (5) already shows the interesting property that after the switching point $t = \tau$, both α_1 and α_2 appear. Expanding the MSD at long time $t \gg \tau$, we find

$$\langle X^2(t) \rangle \sim (\alpha_1 \tau) t^{\alpha_1-1} + t^{\alpha_2}. \quad (6)$$

Fig. 2 shows the time dependence of the MMFBM-MSD for both step-like and sigmoid protocols, showing perfect agreement with the predicted asymptotic behavior. In (6), as long as $\alpha_2 > \alpha_1 - 1$, the second exponent will eventually dominate the MSD scaling. However, when

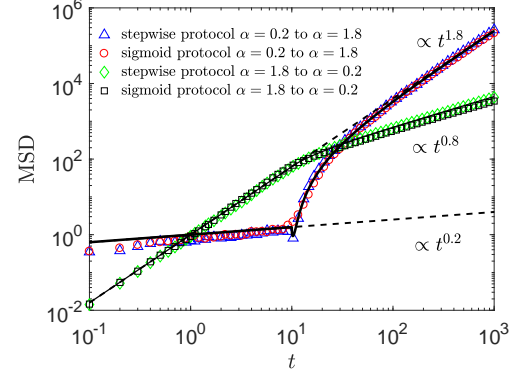


Figure 2: MSD for MMFBM $X(t)$ (1) for step-like and smooth protocol $\alpha(t)$ for two combinations of α_1 and α_2 (see legend). Full lines represent Eq. (5), symbols represent stochastic simulations. A comparison with MFBM is shown in Fig. S2 [72].

$\alpha_1 > 1 + \alpha_2$ the MSD exhibits a continued scaling with $\alpha_1 - 1$ (as confirmed in Fig. 2). In other words, the more superdiffusive behavior is dominant asymptotically, albeit with the reduced slope $\alpha - 1$. Qualitatively this result can be understood from the ACVF of fixed- α FGN, $\langle \xi(t) \xi(t + \Delta) \rangle \simeq \Delta^{\alpha-2}$, that decays slower for larger α (and stays constant in the ballistic limit $\alpha = 2$).

ACVF. We now study the ACVF, which is defined as

$$C(t, \Delta) = \langle X^\delta(t) X^\delta(t + \Delta) \rangle \quad (7)$$

with the increments $X^\delta(t) = X(t + \delta) - X(t)$. First we consider short t , i.e., the first increment $X^\delta(t)$ in (7) is taken before the switching time τ of $\alpha(t)$ in (3). Obviously, when also $t + \Delta < \tau$, the ACVF is the same as for RL-FBM with exponent α_1 and MFBM (Eq. (S10) [72]). This result explicitly depends on both t and Δ , due to the non-stationarity of RL-FBM. When $t = 0$ and $\delta \ll \tau$,

$$C(0, \Delta)_{\Delta < \tau} \sim \frac{\alpha_1(\alpha_1 - 1)\delta^{(\alpha_1+3)/2}}{\alpha_1 + 1} \Delta^{(\alpha_1-3)/2}. \quad (8)$$

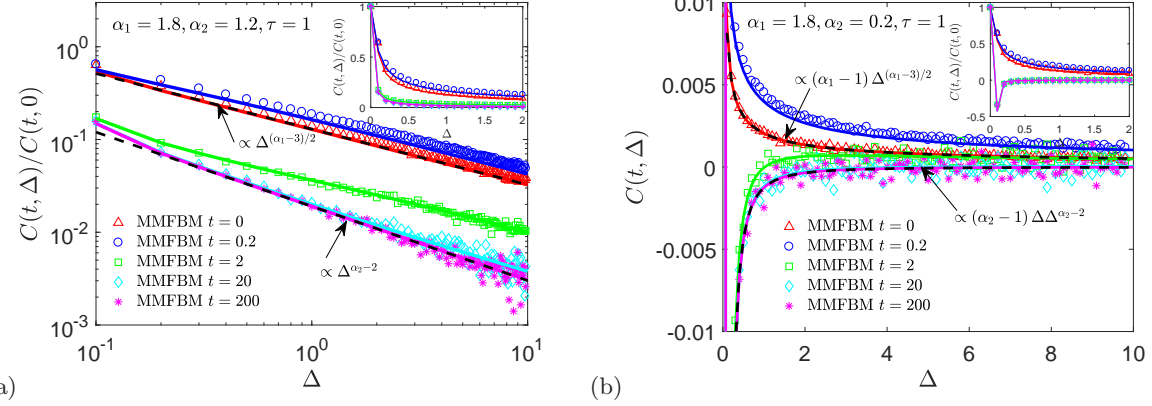


Figure 3: Numerical evaluations (lines) and simulations (symbols) for the ACVF $C(t, \Delta)$ at different times for MMFBM (1) with switching time $\tau = 1$ (a): $\alpha_1 = 1.8, \alpha_2 = 1.2$; (b): $\alpha_1 = 1.8, \alpha_2 = 0.2$. The inset in panel (b) shows the numerically obtained form close to $\Delta = 0$, demonstrating the antipersistence at long times t , when $\alpha_2 = 0.2$ becomes the dominant contribution.

Interestingly, when we correlate increments from before and after the switching time τ , $t + \Delta > \tau$, the MFBM-ACVF (S11) depends on both α_1 and α_2 , while for MMFBM the ACVF is exactly that of *unswitched* RL-FBM and solely depends on α_1 . I.e., for $t = 0$ we recover the form (8) with $\Delta > \tau$. In fact, this result is not surprising. MFBM after the switching is fully independent of the process before the switching, and thus both exponents occur in the ACVF. For MMFBM, in contrast, the process right after the switching event is still dominated by the memory from the evolution before the switching. Consequently, the sole occurrence of α_1 is indeed meaningful. At intermediate times, the MMFBM-ACVF depends on both α_1 and α_2 , as expected (see (S13)). The result needs to be evaluated numerically. However, in the limit $t \rightarrow \infty$, we expect the ACVF to forget about its history and solely depend on α_2 , which is indeed fulfilled,

$$C(\infty, \Delta) = \frac{\alpha_2(\alpha_2 - 1)\Gamma^2((\alpha_2 + 1)/2)\delta^2}{2\Gamma(\alpha_2)\sin(\pi\alpha_2/2)} \Delta^{\alpha_2-2}. \quad (9)$$

Fig. 3 depicts different scenarios for the ACVF (7). Nice agreement between stochastic simulations and the theoretical results is observed. Fig. S3 shows further cases.

PDF. The PDF $P_1(x, t)$ of MMFBM for $t \leq \tau$ is Gaussian. To compute the PDF $P_2(x, t)$ after the crossover, we separate the process into two parts, that are both Gaussian. The PDF of the full process is obtained as

$$P(x, t) = \int_{-\infty}^{\infty} P_1(x_0, \tau) P_2(x - x_0, t - \tau) dx_0 = \frac{\exp(-x^2/[2(t^{\alpha_1} - (t - \tau)^{\alpha_1} + (t - \tau)^{\alpha_2})])}{\sqrt{2\pi(t^{\alpha_1} - (t - \tau)^{\alpha_1} + (t - \tau)^{\alpha_2})}}, \quad (10)$$

which is again a Gaussian process. MMFBM remains Gaussian for any protocol $\alpha(t)$ of the memory exponent.

Local regularity. The self-similarity of a process determines its fractal (Hausdorff) graph dimension [87].

For a Gaussian process it is determined by the semivariogram (structure function) $\gamma_t(\delta) = \langle (X^\delta(t))^2 \rangle$. When $\gamma_t(\delta) \sim D_t \delta^\alpha$, the fractal graph dimension is $2 - \alpha/2$. This also holds for non-stationary increment processes such as RL-FBM [88]. For MMFBM with protocol (3) for $t < \tau$, $X(t)$ is identical to RL-FBM, so this part of the trajectory has fractal dimension $2 - \alpha_1/2$. After the switch it can be shown that the trajectory has fractal dimension $2 - \alpha_2/2$. For any graph containing a piece before and after τ , the lower fractional index and thus the higher fractal dimension dominates [89].

Conclusions. FBM is a widely used process to describe anomalous diffusion in soft- and bio-matter systems. It is characterized by long-ranged, positive or negative correlations in time. Yet many real-world systems exhibit changes in the anomalous diffusion exponent (and thus the memory exponent modulating the correlations in the motion) as function of time. Prime examples include environments, in which particles cross between areas of different viscoelastic properties or when the degree of crowding is controlled. Cargo being pulled intermittently by molecular motors switch between sub- and superdiffusion in cells, and search strategies of birds with correlated increments may vary over time as they switch their motion mode in response to the environment, daytime, or season. In finance the instantaneous degree of roughness of the trading data may vary during the daily rhythm, following interventions in the market, or due to longer-lasting events such as pandemics, wars, or vacation times. Long-range correlated processes such as viscoelastic anomalous diffusion necessarily feature effects of memory of the entire dynamics in physical observables such as the MSD or the ACVF, both of which can be measured.

We here introduced MMFBM as a generalization of FBM to a deterministic form $\alpha(t)$ of the memory exponent. In the correlation integral $\alpha(s)$ locally modulates the Wiener increments $dB(s)$ and thus contributes to the

correlation history of the process. The MSD, and the ACVF of MMFBM exhibit crossovers carrying explicit information from the process prior to switching. This contrasts MFBM, which resets the previous history globally, as seen in the MSD $\langle x^2(t) \rangle \simeq t^{\alpha(t)}$, that solely depends on the instantaneous value of α at process time t . While this reset of correlation history is irrelevant when discussing the instantaneous roughness of a trajectory, for a physical process with long-range correlations this point is crucial when the correlations are directly probed, e.g., in single particle tracking experiments. Here, MMFBM appears physically consistent. We hope that MMFBM will find wide use in soft- and bio-matter systems, finance, ecology, etc. MMFBM will also extend the arsenal of generalized stochastic processes in data analysis [35, 36].

Our discussion was based on non-stationary RL-FBM. MMFBM is thus useful for the description of typical physical systems initiated at $t = 0$ that first have to equilibrate. We demonstrated that at sufficiently long times asymptotic stationarity is restored. It will be interesting to see how MMFBM is modified in the fully stationary limit, i.e., generalizing Mandelbrot-van Ness FBM for systems, that are equilibrated at the start of the measurement. We note that apart from using a purely time-dependent protocol $\alpha(t)$ corresponding to deterministic modifications of the system, it will be interesting to consider scenarios of space-varying scaling exponents in a heterogeneous, quenched system, as well as to combine a protocol $\alpha(t)$ with a time dependence of the (generalized) diffusion coefficients as observed in [49]. Moreover, non-Gaussian extensions of MMFBM should be studied, as well as effects of cutoffs or tempering [90] of the correlations. Finally it should be studied how the non-standard behavior of FBM [91, 92] next to boundaries is modified for MMFBM, relevant, e.g., for growing serotonergic fibers in inhomogeneous brain environments [93].

We acknowledge support from German Science Foundation (DFG grant ME 1535/12-1) and NSF-BMBF CRCNS (grant 2112862/STAXS). AVC acknowledges support by the Polish National Agency for Academic Exchange (NAWA). AW was supported by the Polish National Center of Science (Opus 2020/37/B/HS4/00120). KB acknowledges support through Beethoven Grant DFG-NCN 2016/23/G/ST1/04083.

[1] C. Manzo and M. F. Garcia-Parajo, *Rep. Prog. Phys.* **78**, 124601 (2015).
[2] E. Barkai, Y. Garini, and R. Metzler, *Phys. Today* **65**(8), 29 (2012).
[3] M. J. Saxton, *Biophys. J.* **81**, 2226 (2001).
[4] F. Höfling and T. Franosch, *Rep. Prog. Phys.* **76**, 046602 (2013).
[5] J. Szymanski and M. Weiss, *Phys. Rev. Lett.* **103**, 038102 (2009).
[6] J.-H. Jeon, N. Leijnse, L. B. Oddershede, and R. Metzler, *New J. Phys.* **15**, 045011 (2013).
[7] S. C. Weber, A. J. Spakowitz, and J. A. Theriot, *Phys. Rev. Lett.* **104**, 238102 (2010).
[8] T. J. Lampo, S. Stylianidou, M. P. Backlund, P. A. Wiggins, and A. J. Spakowitz, *Biophys. J.* **112**, 532 (2017).
[9] J.-H. Jeon et al., *Phys. Rev. Lett.* **106**, 048103 (2011).
[10] M. Magdziarz, A. Weron, K. Burnecki and J. Klafter, *Phys. Rev. Lett.* **103**, 180602 (2009).
[11] I. Bronstein et al., *Phys. Rev. Lett.* **103**, 018102 (2009).
[12] A. Caspi, R. Granek, and M. Elbaum, *Phys. Rev. Lett.* **85**, 5655 (2000).
[13] G. Seisenberger et al., *Science* **294**, 1929 (2001).
[14] K. J. Chen, B. Wang, and S. Granick, *Nature Mat.* **14**, 589 (2015).
[15] A. V. Weigel, B. Simon, M. M. Tamkun, and D. Krapf, *Proc. Natl. Acad. Sci. USA* **108**, 6438 (2011).
[16] W. He et al., *Nat. Comm.* **7**, 11701 (2016).
[17] C. Manzo et al., *Phys. Rev. X* **5**, 011021 (2015).
[18] M. J. Skaug, L. Wang, Y. Ding, and D. K. Schwartz, *ACS Nano* **9**, 2148 (2015).
[19] J.-H. Jeon, H. Martinez-Seara Monne, M. Javanainen, and R. Metzler, *Phys. Rev. Lett.* **109**, 188103 (2012).
[20] J.-H. Jeon, M. Javanainen, H. Martinez-Seara, R. Metzler, and I. Vattulainen, *Phys. Rev. X* **6**, 021006 (2016).
[21] E. Yamamoto, T. Akimoto, A. Mitsutake, and R. Metzler, *Phys. Rev. Lett.* **126**, 128101 (2021).
[22] X. Hu, L. Hong, M. Dean Smith, T. Neusius, and J. C. Smith, *Nature Phys.* **12**, 171 (2016).
[23] S. Hapca, J. W. Crawford, and I. M. Young, *J. R. Soc. Interface* **6**, 111 (2009).
[24] K. C. Leptos, J. S. Guasto, J. P. Gollub, A. I. Pesci, and R. E. Goldstein, *Phys. Rev. Lett.* **103**, 198103 (2009).
[25] A. G. Cherstvy, O. Nagel, C. Beta, and R. Metzler, *Phys. Chem. Chem. Phys.* **20**, 23034 (2018).
[26] N. E. Humphries et al., *Nature* **465**, 1066 (2010).
[27] D. W. Sims, N. E. Humphries, N. Hu, V. Medan, and J. Berni, *eLife* **8**, e50316 (2019).
[28] R. Nathan et al., *Science* **375**, eabg1780 (2022).
[29] O. Vilk et al., *Phys. Rev. X* **12**, 031005 (2022).
[30] O. Vilk et al., *Phys. Rev. Res.* **4**, 033055 (2022).
[31] N. G. van Kampen, *Stochastic processes in physics and chemistry* (North Holland, Amsterdam, 1981).
[32] J.-P. Bouchaud and A. Georges, *Phys. Rep.* **195**, 127 (1990).
[33] R. Metzler, J.-H. Jeon, A. G. Cherstvy, and E. Barkai, *Phys. Chem. Chem. Phys.* **16**, 24128 (2014).
[34] I. M. Sokolov, *Soft Matter* **8**, 9043 (2012).
[35] G. Muñoz-Gil et al., *Nature Comm.* **12**, 6253 (2021).
[36] H. Seckler and R. Metzler, *Nat. Commun.* **13**, 6717 (2022).
[37] M. Levin, G. Bel, and Y. Roichman, *J. Chem. Phys.* **154**, 144901 (2021).
[38] I. Y. Wong et al., *Phys. Rev. Lett.* **92**, 178101 (2004).
[39] A. Díez Fernandez, P. Charchar, A. G. Cherstvy, R. Metzler, and M. W. Winn, *Phys. Chem. Chem. Phys.* **22**, 27955 (2020).
[40] M. S. Song, H. C. Moon, J.-H. Jeon, and H. Y. Park, *Nature Comm.* **9**, 344 (2018).
[41] T. H. Solomon, E. R. Weeks, and H. L. Swinney, *Phys. Rev. Lett.* **71**, 3975 (1993).
[42] T. Geisel and S. Thomae, *Phys. Rev. Lett.* **52**, 1936 (1984).

[43] A. N. Kolmogorov, C. R. (Doklady) Acad. Sci. URSS (N. S.) **26**, 115 (1940).

[44] B. B. Mandelbrot and J. W. van Ness, SIAM Rev. **10**, 422 (1968).

[45] H. Qian, in *Processes with long-range correlations: theory and applications*, edited by G. Rangarajan and M. Z. Ding, Lecture Notes in Physics vol 621 (Springer, New York, 2003).

[46] W. H. Deng and E. Barkai, Phys. Rev. E **79**, 011112 (2009).

[47] J. F. Réverey et al., Sci. Rep. **5**, 11690 (2015).

[48] D. Krapf et al., Phys. Rev. X **9**, 011019 (2019).

[49] A. Sabri, X. Xu, D. Krapf, and M. Weiss, Phys. Rev. Lett. **125**, 058101 (2020).

[50] Z. R. Fox, E. Barkai, and D. Krapf, Nat. Comm. **12**, 6162 (2021).

[51] F. Comte and E. Renault, Math. Fin. **8**, 291 (1998).

[52] J. Gatheral, T. Jaisson, and M. Rosenbaum, Quant. Fin. **18**, 933 (2018).

[53] B. Wang, J. Kuo, S. C. Bae, and S. Granick, Nat. Mater. **11**, 481 (2012).

[54] Y. Lanoiselée, N. Moutal, and D. S. Grebenkov, Nat. Commun. **9**, 4398 (2018).

[55] J. Ślęzak, R. Metzler, and M. Magdziarz, New J. Phys. **20**, 023026 (2018).

[56] A. V. Chechkin, F. Seno, R. Metzler, and I. M. Sokolov, Phys. Rev. X **7**, 021002 (2017).

[57] M. V. Chubynsky and G. W. Slater, Phys. Rev. Lett. **113**, 098302 (2014).

[58] W. Wang et al., J. Phys. A **53**, 474001 (2020).

[59] W. Wang, F. Seno, I. M. Sokolov, A. V. Chechkin, and R. Metzler, New J. Phys. **22**, 083041 (2020).

[60] D. Han et al., eLife **9**, e52224 (2020).

[61] M. Balcerek, K. Burnecki, S. Thapa, A. Wyłomańska, and A. Chechkin, Chaos **32**, 093114 (2022).

[62] P. D. Odermatt et al. eLife **10**, 64901 (2021).

[63] A. J. Barlow et al., Proc. Roy. Soc. A **327**, 403 (1972).

[64] J. Caspers et al., E-print arXiv:10820.0122.

[65] F. Etoc et al., Nat. Mat. **17**, 740 (2018).

[66] I. Heller et al., Nat. Meth. **10**, 910 (2013).

[67] D. Robert, T. Nguyen, F. Gallet, and C. Wilhelm, PLoS ONE **5**, e10046 (2010).

[68] I. Goychuk, V. O. Kharchenko, and R. Metzler, Phys. Chem. Chem. Phys. **16**, 16524 (2014).

[69] P. Lévy, in *Random functions: general theory with special reference to Laplacian random functions* (University of California Press, Berkeley, 1953).

[70] We here use a dimensionless notation. To restore physical units the associated prefactor $\alpha(s)$ in Eq. (1) can be replaced by the form $[K_{\alpha(s)}] = \alpha(s)\ell_0^2/t_0^{\alpha(s)}$. Dimensionality can then be removed by setting the length scale ℓ_0 and the time scale t_0 to unity. The specific choice of the dimensionless prefactor $\alpha(s)$ in this expression for $K_{\alpha(s)}$ allows a compact notation and to illustrate the most essential features of the MMFBM model.

[71] A. V. Chechkin, R. Gorenflo, and I. M. Sokolov, Phys. Rev. E **66**, 046129 (2002).

[72] Supplementary Material

[73] A. Ayache, C. Esser, and J. Hamonier, Risk Decis. Anal. **7**, 5 (2018).

[74] A. Philippe, D. Surgailis, and M.-C. Viano, Theory Prob. Appl. **52**, 651 (2008).

[75] D. Surgailis, Stoch. Proc. Appl. **118**, 171 (2008).

[76] A. Ayache and F. Bouly, Stoch. Proc. Appl. **146**, 143 (2022).

[77] S. A. Stoev and M. S. Taqqu, Stoch. Proc. Appl. **116**, 200 (2006).

[78] A. Ayache and J. Lévy-Véhel, Statist. Infer. Stoch. Proc. **3**, 7 (2000).

[79] M. Balcerek and K. Burnecki, Entropy **22**, 1403 (2020).

[80] D. Szarek, I. Jabłoński, D. Krapf, and A. Wyłomańska, Chaos **32**, 083148, (2022).

[81] M. Li, S. C. Lim, B.-J. Hu, and H. Feng, in *Lecture notes in computer science 4488*, edited by Y. Shi, G. Dick van Albada, J. Dongarra, and P. M. A. Sloot (Springer, Berlin, 1987).

[82] J. Lévy-Véhel and R. Riedi, in *Fractals in engineering*, edited by J. Lévy Véhel, E. Lutton, and C. Tricot (Springer, Berlin, 1997).

[83] S. Bianchi, A. Pantanella, and A. Pianese, Quant. Fin. **13**, 1317 (2011).

[84] K. C. Lee, Nonlin. Proc. Geophys. **20**, 97 (2013).

[85] C. Box, *Multifractional Brownian motion and its applications to factor analysis on consumer confidence index*, Senior thesis, Claremont College, 2021.

[86] We note that we choose the additional prefactor $\sqrt{\alpha(t)}$ in the definition of MFBM, compare [73] in agreement with RL-FBM [44]. This choice does not change the fundamental behavior.

[87] K. Falconer, *Fractal geometry* (John Wiley & Sons, Chichester, UK, 1990).

[88] J. Picard, in *Séminaire de Probabilités XLIII*, edited by C. Donati-Martin, A. Lejay, and A. Rouault, Lecture Notes in Mathematics 2006 (Springer, New York, 2011).

[89] W. Wang et al., (unpublished).

[90] D. Molina-Garcia et al., New J. Phys. **20**, 103027 (2018).

[91] T. Vojta et al., Phys. Rev. E **102**, 032108 (2020).

[92] T. Guggenberger, A. Chechkin, and R. Metzler, J. Phys. A **54**, 29LT01 (2021).

[93] S. Janušonis, N. Detering, R. Metzler, and T. Vojta, Front. Comp. Neurosci. **14**, 56 (2020).

[94] M. Abramowitz and I. Stegun, *Handbook of mathematical functions* (Dover, New York, 1972).

**Supplementary Material:
Memory-multi-fractional Brownian motion with continuous correlations**

LÉVY'S RIEMANN-LIOUVILLE-FBM

A well-known representation of fractional Brownian motion (FBM) is attributed by Mandelbrot [44] to Paul Lévy [69]. It is given by the Holmgren-Riemann-Liouville fractional integral [44]

$$B_\alpha(t) = \sqrt{\alpha} \int_0^t (t-s)^{(\alpha-1)/2} dB(s) \quad (\text{S1})$$

$B(t)$ is standard Brownian motion and $\alpha \in (0, 2]$. It is easy to show that the MSD of $B_\alpha(t)$ yields as $\langle B_\alpha^2(t) \rangle = t^\alpha$.

This exact equality follows from the choice of the prefactor in definition (S1) [61].

With the increments of RL-FBM for disjoint intervals $[t, t + \delta]$ and $[t + \Delta, t + \Delta + \delta]$,

$$B_\alpha^\delta(t) = B_\alpha(t + \delta) - B_\alpha(t), \quad B_\alpha^\delta(t + \Delta) = B_\alpha(t + \Delta + \delta) - B_\alpha(t + \Delta), \quad (\text{S2})$$

the ACVF of RL-FBM is given by

$$C_B(t, \Delta) = \langle B_\alpha^\delta(t) B_\alpha^\delta(t + \Delta) \rangle. \quad (\text{S3})$$

For $\Delta \gg \delta$, after some transformations we obtain the ACVF

$$\begin{aligned} C_B(t, \Delta) &\approx \frac{\alpha(\alpha-1)(3-\alpha)\delta^2}{4} \int_0^t q^{(\alpha-1)/2} (q + \Delta)^{(\alpha-5)/2} dq + \frac{\alpha(\alpha-1)\delta}{2} \int_t^{t+\delta} q^{(\alpha-1)/2} (q + \Delta)^{(\alpha-3)/2} dq \\ &= \frac{\alpha(\alpha-1)(3-\alpha)\delta^2}{4} \mathbb{B} \left(\frac{t/\Delta}{1+t/\Delta}, \frac{\alpha+1}{2}, 2-\alpha \right) \Delta^{\alpha-2} + \frac{\alpha(\alpha-1)\delta}{2} \int_t^{t+\delta} q^{(\alpha-1)/2} (q + \Delta)^{(\alpha-3)/2} dq, \end{aligned} \quad (\text{S4})$$

where $\mathbb{B}(z; a, b)$ is the incomplete Beta function [94]

$$\mathbb{B}(z; a, b) = \int_0^z s^{a-1} (1-s)^{b-1} ds. \quad (\text{S5})$$

RL-FBM has non-stationary increments at any given time t , i.e., it does not solely depend on the time lag Δ .

MFBM

A direct generalization of FBM to multifractional Brownian motion (MFBM) is to replace α by an explicitly time-dependent function $\alpha(t)$. In comparison to mathematical literature (see, e.g., [73, 77, 78]) we base the generalization on RL-FBM (S1) with the square-root prefactor,

$$Y(t) = \sqrt{\alpha(t)} \int_0^t (t-s)^{(\alpha(t)-1)/2} dB(s). \quad (\text{S6})$$

In MFBM, the long-range correlations are reset, as only the instantaneous value of α at time t is considered in (S6), and the MSD scales like

$$\langle Y^2(t) \rangle = t^{\alpha(t)}. \quad (\text{S7})$$

Trajectories for MFBM and MMFBM for a step-like protocol are shown in Fig. S1. Evidently, the path of the conventional MFBM has a discontinuous jump at the switching time while the path of MMFBM is continuous.

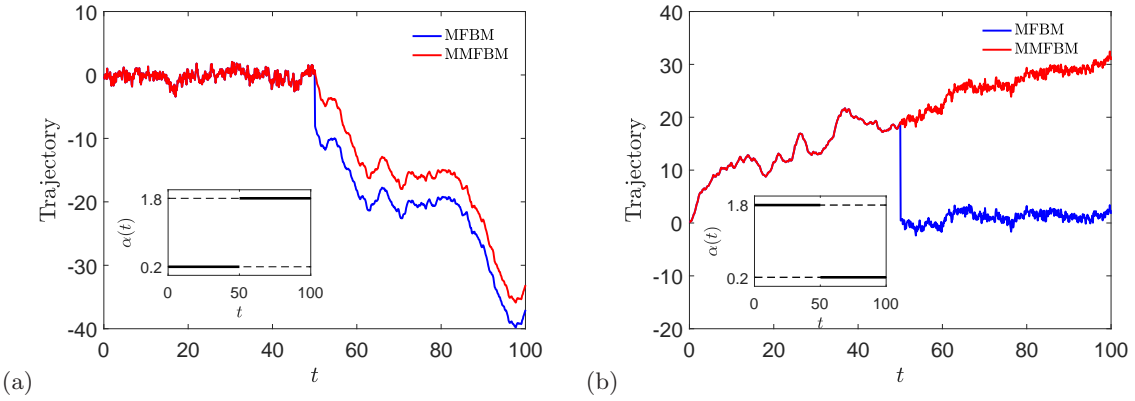


Figure S1: Trajectories for MMFBM (1) and MFBM (S6) for a stepwise protocol for $\alpha(t)$ with switching time $\tau = 50$ and (a): $\alpha_1 = 0.2, \alpha_2 = 1.8$; (b): $\alpha_1 = 1.8, \alpha_2 = 0.2$. In each panel both trajectories are based on the same realization of the underlying Wiener process. The time series of the parental Wiener increments is also the same as for Fig. 1, in which we show trajectories produced by smooth sigmoid variants (S17) of protocol (2).

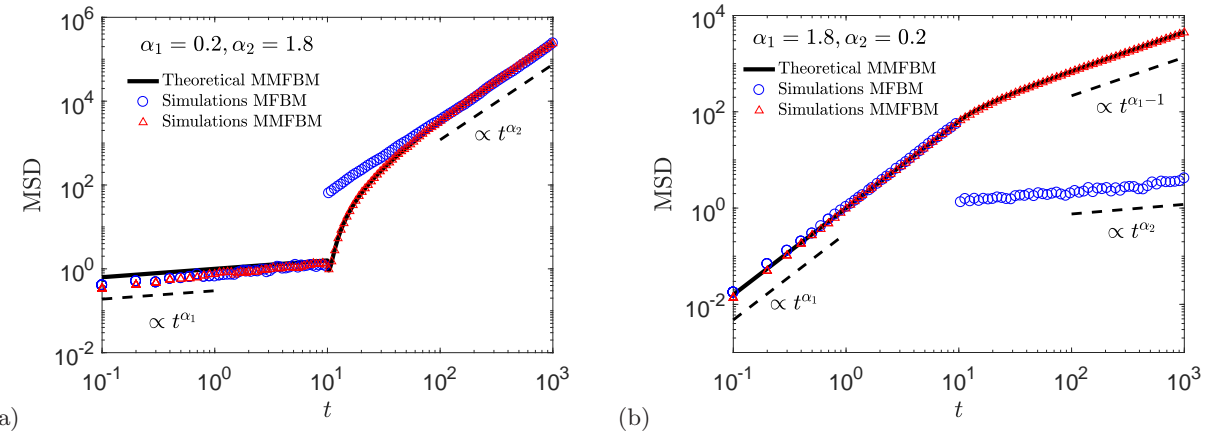


Figure S2: MSDs for MFB and MMFBM with switching time $\tau = 10$: (a) $\alpha_1 = 0.2, \alpha_2 = 1.8$, (b) $\alpha_1 = 1.8, \alpha_2 = 0.2$. The theoretical MSD (5) of MMFBM is represented by solid black curves. Note that the MMFBM-MSD is always continuous, while the derivative is continuous when $\alpha_1, \alpha_2 > 1$. For MFBM the MSD is always discontinuous.

MSD OF MFBM

The MSD of MFBM (S6) with step-like anomalous diffusion exponent jumping from α_1 to α_2 at $t = \tau$, yields in the form

$$\langle Y^2(t) \rangle = \begin{cases} t^{\alpha_1}, & t \leq \tau \\ t^{\alpha_2}, & t > \tau \end{cases} \quad (\text{S8})$$

Indeed, for $t > \tau$, solely the value α_2 appears, due to the reset correlations of MFBM. The MSDs for MFBM and MMFBM are displayed in Figs. S2 along with stochastic simulations.

ACVF FOR MMFBM AND MFBM

We define the increment of MMFBM as $X^\delta(t) = X(t + \delta) - X(t)$. The ACVF is given by $C_X(t, \Delta) = \langle X^\delta(t) X^\delta(t + \Delta) \rangle$, where the time step δ is taken to be small, $\delta \ll \Delta, \tau$. Similarly, the ACVF for MFBM (S6) is $C_Y(t, \Delta)$. In the limits of short and long times t analytical results can be obtained for the ACVFs for step-like protocol of α .

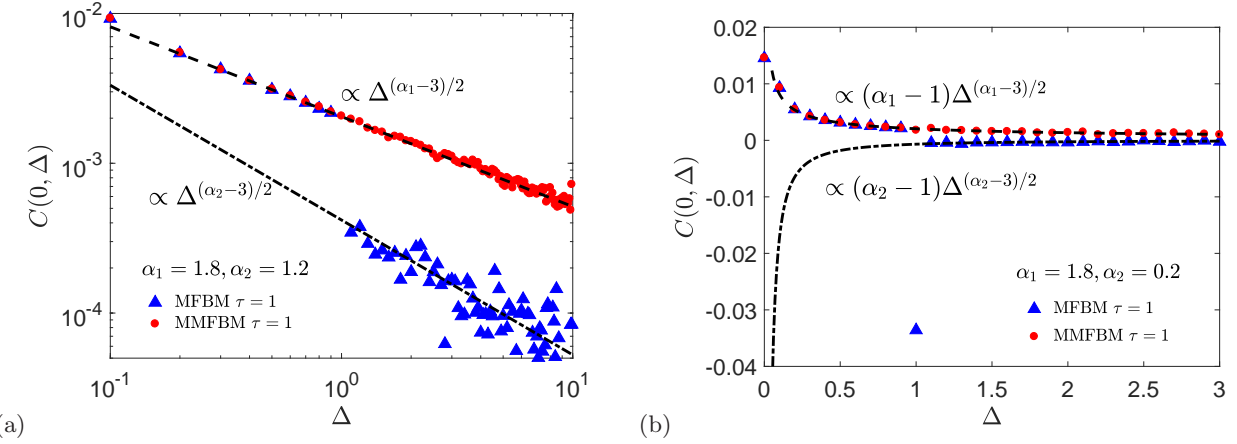


Figure S3: ACVF for MFBM and MMFBM with switching time $\tau = 1$. The theoretical ACVF of classic MFBM (S9) switches to (S12) when the anomalous diffusion exponent switches. The ACVF $C(0, \Delta)$ of MMFBM (S9), (S10) remains the same depending on α_1 .

Short time limit of the ACVF

We first consider $t < \tau$. Then we distinguish two cases:

(i) When $t + \Delta < \tau$ we have the same ACVF (S4) as that of RL-FBM. In particular, when $t = 0$ and $\Delta \gg \delta$, we have the ACVF for both MMFBM and MFBM according to

$$C_X(0, \Delta)_{\Delta < \tau} = C_Y(0, \Delta)_{\Delta < \tau} = C_B(0, \Delta | \alpha_1) \sim \frac{\alpha_1(\alpha_1 - 1)\delta^{(\alpha_1+3)/2}}{\alpha_1 + 1} \Delta^{(\alpha_1-3)/2}. \quad (\text{S9})$$

(ii) When $t + \Delta > \tau$, the increment $X^\delta(t + \Delta)$ of MMFBM is measured after switching and $X^\delta(t)$ before switching. Multiplying the two increments and averaging over the realizations, the ACVF is independent of α_2 and coincides with the results (S4) of RL-FBM. For $t = 0$ and $\Delta \gg \delta$,

$$C_X(0, \Delta)_{\Delta > \tau} \sim \frac{\alpha_1(\alpha_1 - 1)\delta^{(\alpha_1+3)/2}}{\alpha_1 + 1} \Delta^{(\alpha_1-3)/2}. \quad (\text{S10})$$

In contrast, for MFBM the increment after switching is given by $Y(t + \Delta + \delta) - Y(t + \Delta)$ and the ACVF for MFBM depends on both α_2 and α_1 ,

$$\begin{aligned} C_Y(t, \Delta)_{t+\Delta > \tau} &= \frac{\sqrt{\alpha_1 \alpha_2}(\alpha_2 - 1)(3 - \alpha_2)\delta^2}{4} \mathbb{B}\left(\frac{t}{\Delta}; \frac{\alpha_1 + 1}{2}, 2 - \frac{\alpha_1 + \alpha_2}{2}\right) \Delta^{(\alpha_1+\alpha_2)/2-2} \\ &+ \frac{\sqrt{\alpha_1 \alpha_2}(\alpha_2 - 1)\delta}{2} \int_t^{t+\delta} q^{(\alpha_1-1)/2} (q + \Delta)^{(\alpha_2-3)/2} dq. \end{aligned} \quad (\text{S11})$$

When $t = 0$ and $\Delta \gg \delta$, we have the MFBM-ACVF

$$C_Y(0, \Delta)_{\Delta > \tau} \sim \frac{\sqrt{\alpha_1 \alpha_2}(\alpha_2 - 1)\delta^{(\alpha_1+3)/2}}{\alpha_1 + 1} \Delta^{(\alpha_2-3)/2}. \quad (\text{S12})$$

The ACVF of MMFBM and MFBM are shown in Fig. S3. When the anomalous diffusion exponent switches from α_1 to α_2 , the ACVF for $t = 0$ of MFBM crosses over from the scaling $\Delta^{(\alpha_1-3)/2}$ to $\Delta^{(\alpha_2-3)/2}$, while the MMFBM-ACVF retains the scaling $\Delta^{(\alpha_1-3)/2}$. This clearly shows the uninterrupted memory of MMFBM, in contrast to MFBM.

Long time limit of the ACVF

When $t > \tau$ both increments are observed after the switching of α . After some transformations we obtain the ACVF

$$C_X(t, \Delta) = f\left(\alpha_1, \frac{t}{\Delta}\right) - f\left(\alpha_1, \frac{t-\tau}{\Delta}\right) + f\left(\alpha_2, \frac{t-\tau}{\Delta}\right) + g\left(\alpha_1, \frac{t}{\Delta}\right) - g\left(\alpha_1, \frac{t-\tau}{\Delta}\right) + g\left(\alpha_2, \frac{t-\tau}{\Delta}\right), \quad (\text{S13})$$

where

$$f(\alpha, s) = \frac{\alpha(\alpha-1)\delta^2}{2} s^{(\alpha-1)/2} (1+s)^{(\alpha-3)/2} \Delta^{\alpha-2}, \quad g(\alpha, s) = \frac{\alpha(\alpha-1)(3-\alpha)\delta^2}{4} \mathbb{B} \left(s; \frac{\alpha+1}{2}, 2-\alpha \right) \Delta^{\alpha-2}. \quad (\text{S14})$$

When $t \rightarrow \infty$,

$$C_X(\infty, \Delta) = g(\alpha_2, \infty) = \frac{\alpha_2(\alpha_2-1)\Gamma^2((\alpha_2+1)/2)\delta^2}{2\Gamma(\alpha_2)\sin(\pi\alpha_2/2)} \Delta^{\alpha_2-2}. \quad (\text{S15})$$

For MFBM, the increments depend locally on the Hurst exponents at time t . The ACVF of MFBM is the same as that of FBM with the same α_2 at time t after switching, and when $t \rightarrow \infty$,

$$C_Y(\infty, \Delta) = \frac{\alpha_2(\alpha_2-1)\Gamma^2((\alpha_2+1)/2)\delta^2}{2\Gamma(\alpha_2)\sin(\pi\alpha_2/2)} \Delta^{\alpha_2-2}. \quad (\text{S16})$$

As it should be, at extremely long times beyond the switching time, the ACVFs of RL-FBM, MFBM, and MMFBM converge to the same behavior.

SMOOTH SWITCHING OF ANOMALOUS DIFFUSION EXPONENT

While the stepwise protocol (2) used here simplifies the analytical calculation, it is interesting to consider smooth variations. We here briefly study the exponentially switching anomalous diffusion exponent

$$\alpha(t) = \frac{\alpha_2 - \alpha_1}{1 + \exp(-(t - \tau)/T)} + \alpha_1, \quad (\text{S17})$$

where T is some characteristic time measuring how fast the exponent switches from α_1 to α_2 around $t = \tau$. At short times $t \ll \tau$, we see that $\alpha(t) \approx \alpha_1$ while at long times $t \gg \tau$, $\alpha(t) \approx \alpha_2$. Numerically evaluated trajectories and MSDs for MFBM and MMFBM with smoothly switching exponent (S17) are displayed in Figs. 1 and 2.